Hydrodynamic Performance of Flapping-foil Propulsion in the Influence of Vortices

Xi Zhang, Yu-min Su, Liang Yang and Zhao-li Wang

State Key Laboratory of Autonomous Underwater Vehicle, Harbin Engineering University, Harbin 150001, China

Abstract: Fish are able to make good use of vortices. In a complex flow field, many fish continue to maintain both efficient cruising and maneuverability. Traditional man-made propulsion systems perform poorly in complex flow fields. With fish-like propulsion systems, it is important to pay more attention to complex flow fields. In this paper, the influence of vortices on the hydrodynamic performance of 2-D flapping-foils was investigated. The flapping-foil heaved and pitched under the influence of inflow vortices generated by an oscillating D-section cylinder. A numerical simulation was run based the finite volume method, using the computational fluid dynamics (CFD) software FLUENT with Reynolds-averaged Navier-Stokes (RANS) equations applied. In addition, dynamic mesh technology and post processing systems were also fully used. The calculations showed four modes of interaction. The hydrodynamic performance of flapping-foils was analyzed and the results compared with experimental data. This validated the numerical simulation, confirming that flapping-foils can increase efficiency by absorbing energy from inflow vortices.

Keywords: flapping-foil; vortex; numerical simulation; hydrodynamic performance; save energy

Article ID: 1671-9433(2010)02-0213-07

1 Introduction

When fish swims, vortices are generated from fish body. These vortices affect the propulsive performance of fish tail largely. In the study of fish-like propulsion systems, the fish tail is simplified as a rigid or flexible flapping-foil. So it's important to study the propulsive performance of flapping-foil in the complex flow field.

Streitlien and Triantafyllou (1996) applied potential method to study the performance of a 2D flapping-foil in the flow field in the influence of point vortices. He found that the flapping-foil could absorb the energy of vortices so that the propulsive efficiency was increased. Gopalkrishnan *et al.*(1994) made an experiment on the flapping-foil which was in the Karman vortex street. Interaction modes between inflow vortices and vortices generated by flapping-foil motion were obtained in the experiment. The propulsive efficiencies of different modes were also analyzed. Beal DN's experiment indicated that the flapping-foil could absorb energy from income vortices to strengthen the thrust force. Liao *et al.*(2004) conducted an investigation in force characteristics of a stationary foil in the wake of a stationary circular cylinder. It is found that a preferred vortex shedding frequency of the foil is synchronized with that of the circular cylinder.

In this paper CFD method was used to analyze the hydrodynamic performance of 2-D flapping-foil in the influence of inflow vortices. Interaction modes between inflow vortices and generated vortices were obtained. The performance in different modes was analyzed and compared.

The D-section cylinder was used as a vortex generator. Many researchers including Bearman(1984), Sarpkaya(1979),. Stansby (1976) and Williamson(1988) have studied oscillating cylinders. Few people have studied D-section cylinders. Simmon studied the turbulent wake of a D-section cylinder. He found that the wake is well organized staggered array of oppositely signed vortices.

A number of studies have been experimentally and numerically performed on the flapping-foil. Triantafyllou experimentally proved that the wake structure of flapping-foil make influence on the hydrodynamic performance. Laura studied the wake structure of flapping-foil by means of the numerical solution of the vorticity equation. Wang studied the problem by means of incompressible 2-D Navier-Stokes equation.

2 Calculation model

In this paper, the performance of flapping-foil in the influence of inflow vortices was studied. Inflow vortices were generated by an oscillating D-section cylinder in the front of flapping-foil. The interaction mode between inflow vortices and foil vortices was controlled by distance from center of the D-section cylinder to pivot point of the flapping-foil.
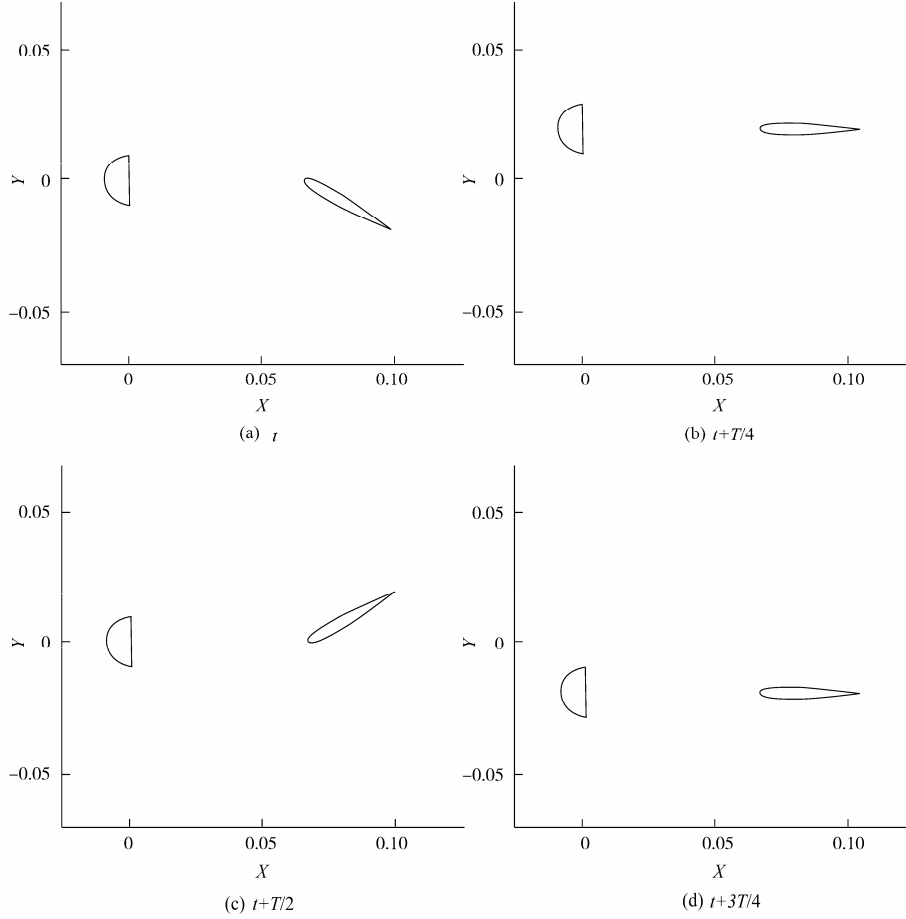
2.1 The motion of the model

The D-section cylinder's motion is described as below:

$$y = A_d \sin(2\pi f_d t) \qquad (1)$$

(a) t

(b) $t+T/4$

(c) $t+T/2$

(d) $t+3T/4$

Fig.1 The cylinder-foil tandem motion in one cycle

In the formula (1), A_d represents the amplitude of heave translation. f_d represents the frequency of heave translation. The flapping-foil's motion is described as below:

$$y = A_f \sin(2\pi f t)$$
$$\theta = \theta_0 \sin(2\pi f t + \varphi) \qquad (2)$$

In the formula (2), A_f represents the amplitude of heave translation, θ_0 represents the amplitude of pitch rotation, f represents the frequency of flapping motion. φ represents the phase angle of flapping motion between heave translation and pitch rotation.

In the cylinder-foil tandem arrangements, $A_f = A_d$, $f_d = f$, $\varphi = 1/2\pi$. The cylinder-foil tandem motion in one cycle is shown in Fig.1.

2.2 Important dimensionless numbers of the model

There are two dimensionless numbers which have influence on the hydrodynamic performance of flapping-foil:

$$Re_d = \frac{V_{ref} \cdot d}{\upsilon} \qquad \sigma = \frac{s}{V_{ref} \cdot T}$$

Re_d is the Reynolds number of D-section cylinder. d represents the diameter of D-section cylinder, V_{ref} the inflow velocity, υ the motion viscosity coefficient of water, σ the distance between the center of D-section cylinder and the pivot point of flapping foil, and T is the motion cycle.

The dimensionless numbers which represent the hydrodynamic performance of flapping-foil are described as below:

$$C_x = \int_l \frac{F_x}{1/2\rho C_0 V_{vef}^2} \, \mathrm{d}l \quad , \quad C_y = \int_l \frac{F_y}{1/2\rho C_0 V_{vef}^2} \, \mathrm{d}l \quad ,$$

$$C_m = \int_l \frac{M_0}{1/2\rho C_0^2 V_{vef}^2} \, \mathrm{d}l$$

C_x represents the thrust force coefficient, C_y the lateral force coefficient, C_m the moment coefficient, the leading edge of

flapping-foil is set as pivot point. C_0 represents the length of chord. ρ is the density of water.

The propulsive efficiency of flapping-foil used by Yang L et al. is described as below:

$$\eta = \frac{\dfrac{1}{T} \cdot \displaystyle\int_0^T \int_l F_x(t) \cdot V_{ref} \, \mathrm{d}l\mathrm{d}t}{\dfrac{1}{T} \cdot \left(\displaystyle\int_0^T \int_l F_y(t) \cdot y'(t) \, \mathrm{d}l\mathrm{d}t + \int_0^T \int_l M_0(t) \cdot \theta'(t) \, \mathrm{d}l\mathrm{d}t \right)}$$

3 Calculation method

3.1 The numerical method

In this paper, 2D incompressible Reynolds-Averaged Navier-Stokes equation based on finite volume method referenced by Wang's book was applied. The whole computing area was divided into different patches. UDF programs were used to describe the motion of the model. SIMPLE arithmetic was applied. The $k - \omega \ sst$ two equations turbulence model was used.

The 2D dynamic triangular unstructured mesh based on spring method was applied. The mesh around D-section cylinder and foil should be denser in order to obtain the interaction process between inflow vortices and foil vortices. The time step must be small enough for the demand of dynamic mesh.

3.2 The validation of numerical method

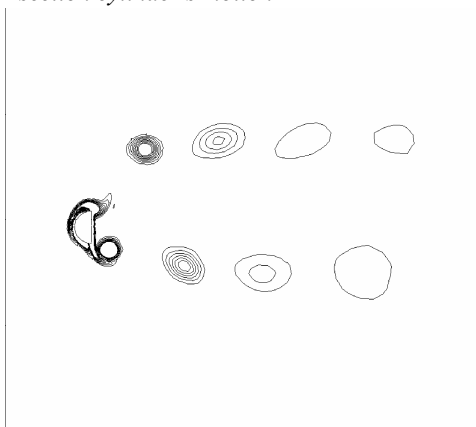*3.2.1 D-section cylinder's motion*

Fig.2 Vortices generated by D-section cylinder motion

Vortices are generated and shedding into downstream continually, which is shown in Fig.2. Vortices which are like Karman Vortex Street are clockwise in one side and counter clockwise in another side. Vortices in the same direction are distributed with approximately the same spacing along *x* axis direction. Vortices in different directions are distributed with approximately the same spacing along *y* axis direction. As the distance between D-section cylinder and the vortex is larger, the vortex decreases continually. In the computing

process, the quality of vortices is excellent downstream away, nearly 8*d* from D-section cylinder. Considering the cylinder-foil tandem motion, the flapping-foil is always less than 8*d* from D-section cylinder. So the D-section cylinder could be used as a vortex-generator.

The diameter of cylinder, *d*=1.91cm. Inflow velocity, V_{ref} =2.82cm/s. The Reynolds number of cylinder, Re_d=540. The dimensionless amplitude $a = \dfrac{2A_d}{d}$, the dimensionless space between vortices in the same direction $\bar{s} = \dfrac{s}{V_{ref} \cdot T}$, the dimensionless space between vortices in different directions, $\bar{h} = \dfrac{h}{d}$.

The calculation results compared with experimental result obtained from Anderson are shown in Figs.3~5 in three conditions of *a* from 1.0 to 3.0 by 1.0 with the same *f*=0.5.
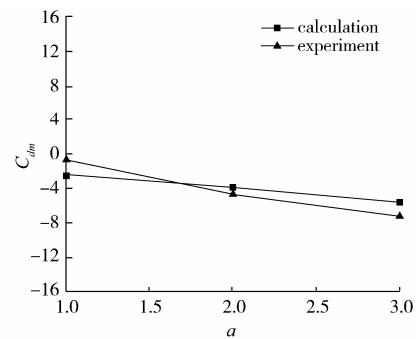

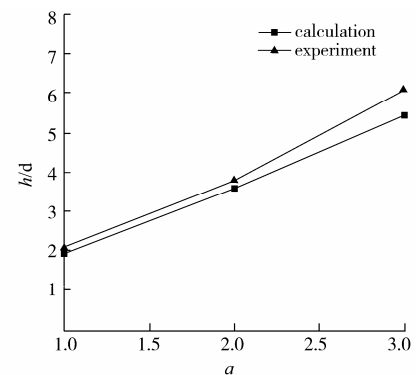**Fig.3 The mean drag force coefficient varies with *a***
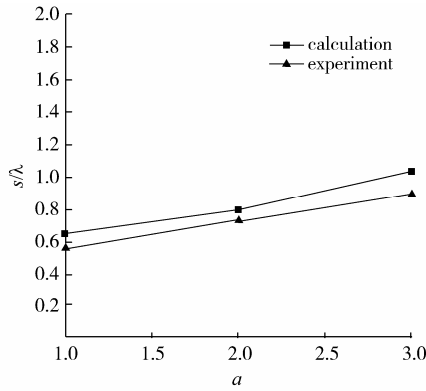

Fig.4 $\bar{h}$ varies with *a*

Fig.5 $\bar{s}$ varies with a

Comparing with the experimental data, the trends of the curves are nearly the same.

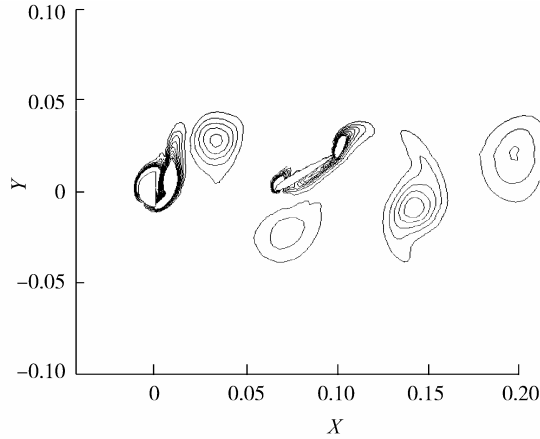*3.2.2 The cylinder-foil tandem motion*

Fig.6 The flapping-foil motion with inflow vortices

The calculation done by Song validates the numerical method. The cylinder-foil tandem motion is shown in Fig.6. The calculation results compared with experimental data are shown in Fig.7 in four conditions of σ from 0.75 to 1.0 by 0.25 with the same f=0.32, Re_d=540, a=2.0, $\theta_0 = 15°$. The trends of the curves are approximately the same.
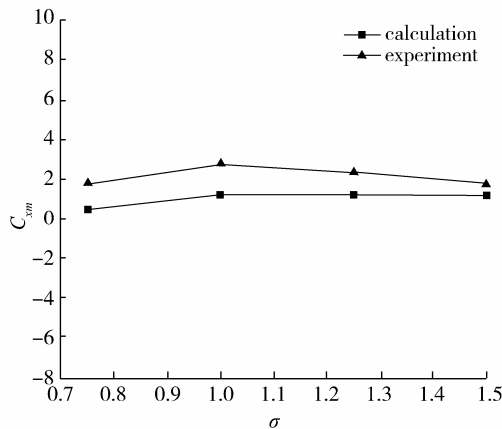

Fig.7 The mean thrust force coefficient varies with σ

4 Results and discussion

4.1 The interaction mode

There are four types of interaction mode which are found in calculation results between inflow vortices and foil vortices.

Mode1: Keep the inflow vortex away from the flapping-foil so as not to interact with the foil vortex.

Mode2: The inflow vortex interacts with the same signed foil leading edge vortex and then they move forward independently. At last they merge into the same signed foil trail edge vortex.

Mode3: The inflow vortex doesn't interact with foil leading edge vortex. At last it merges into the same signed foil trail edge vortex.

Mode4: The inflow vortex interacts with the oppositely signed vortices generated by flapping-foil.

At $\theta_0 = 15°$ and σ from 0.75 to 1.5 by 0.25, the interaction modes between inflow vortices and foil vortices are shown in Table 1. At $\theta_0 = 30°$ and σ from 0.75 to 1.5 by 0.25, the interaction modes between inflow vortices and foil vortices are shown in Table 2.

Table 1 $\theta_0 = 15°$ interaction modes with inflow vortices

σ	Interaction mode with top vortices	Interaction mode with bottom vortices
0.75	Mode2	Mode2
1.0	Mode3	Mode3
1.25	Mode4	Mode4
1.5	Mode2	Mode1

Table 2 $\theta_0 = 30°$ interaction modes with inflow vortices

σ	Interaction mode with top vortices	Interaction mode with bottom vortices
0.75	Mode2	Mode2
1.0	Mode3	Mode3
1.25	Mode4	Mode4
1.5	Mode4	Mode2

4.2 The hydrodynamic performance of flapping-foil in the influence of inflow vortices

4.2.1 The mean thrust force coefficient of flapping-foil in the influence of inflow vortices

The curve of mean thrust force coefficient varying with σ at $\theta_0 = 15°$ is shown in Fig.8. C_{xm} increases first and then decreases with the increase of σ. The change rate of C_{xm} is large with σ from 0.75 to 1.0. And then the change rate becomes small. C_{xm} is the largest at $\sigma = 1.25$.

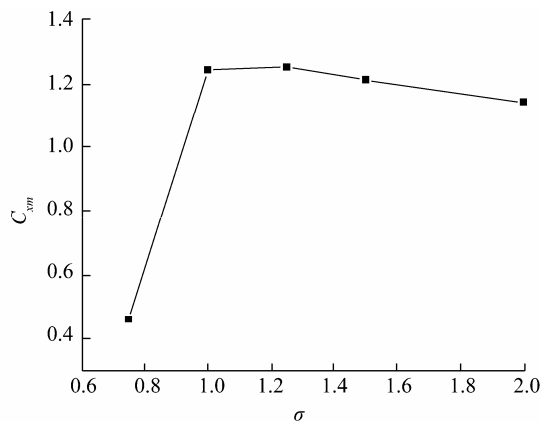At $\sigma = 2.0$ the influence of inflow vortices is very small.

Fig.8 The mean thrust force coefficient at θ=15°

The curve of mean thrust force coefficient varying with σ at θ=30° is shown in Fig.9. C_{xm} increases first and then decreases with the increase of σ. The change rate of C_{xm} is large. C_{xm} is the largest at $\sigma = 1.25$. At $\sigma = 2.0$ the influence of inflow vortices can be ignored.
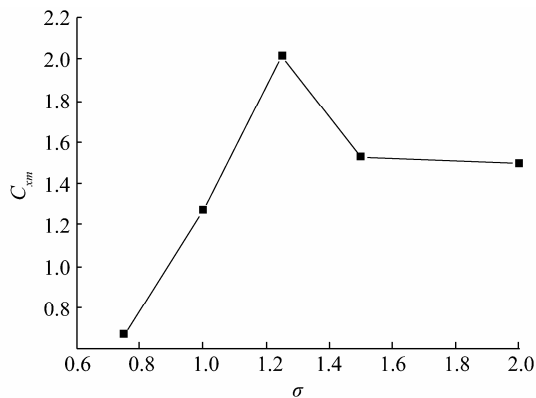

Fig.9 The mean thrust force coefficient at θ=30°

Above all, C_{xm} is largest at $\sigma = 1.25$ and smallest at $\sigma = 0.75$. Connecting with interaction modes, C_{xm} is increased at mode 4 and diminished at mode 2.

4.2.2 The propulsive efficiency and input power of flapping-foil in the influence of inflow vortices

The curves of input power and efficiency varying with σ at $\theta_0 = 15°$ are shown in Fig.10. The input power coefficient at $\sigma = 1.25$ is larger than the one at $\sigma = 2.0$. But efficiency at $\sigma = 1.25$ is smaller. Obviously the inflow vortices absorb energy from the flapping-foil. On the contrary, the input power coefficient at $\sigma = 1.5$ is smaller than the one at $\sigma = 2.0$. But efficiency at $\sigma = 1.5$ is larger. So the flapping-foil could obtain external energy from inflow vortices.
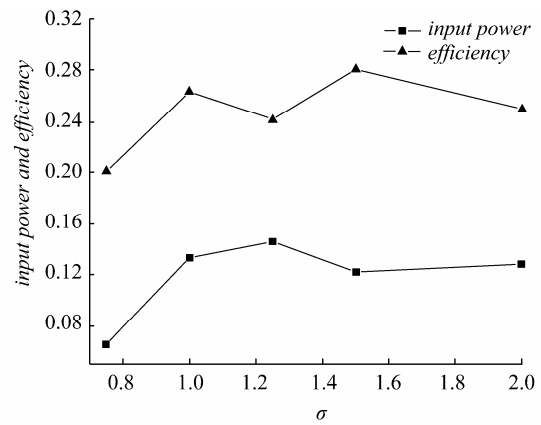

Fig.10 The input power and efficiency at θ=15°

The curves of input power and efficiency varying with σ at $\theta_0 = 30°$ are shown in Fig.11. The input power coefficient at $\sigma = 1.5$ is smaller than the one at $\sigma = 2.0$. But efficiency at $\sigma = 1.5$ is larger. So the flapping-foil could obtain external energy from inflow vortices. Compared with propulsive performance at $\sigma = 1.0$, the input power coefficient is smaller but efficiency larger at $\sigma = 0.75$. So the flapping-foil at $\sigma = 0.75$ is more adaptive for inflow vortices.
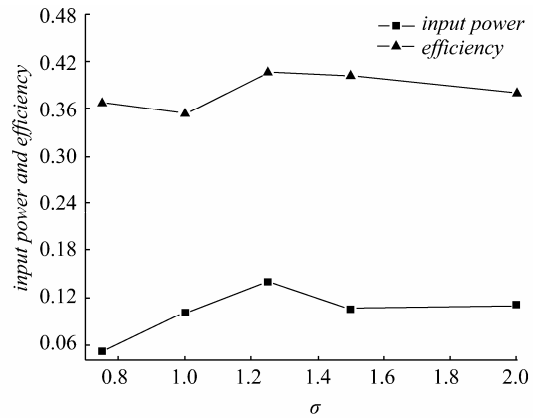

**Fig.11 The input power and efficiency at θ=30°**

Above all, the flapping-foil could absorb energy from inflow vortices at $\sigma = 1.5$. Connecting with interaction modes, the flapping-foil could absorb energy from inflow vortices at mode 2.

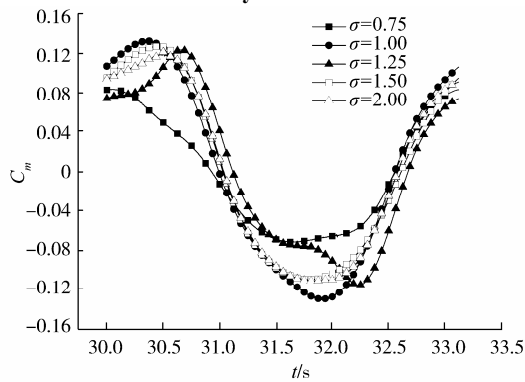*4.2.3 The hydrodynamic coefficients of flapping-foil in the influence of inflow vortices*

The hydrodynamic coefficients of flapping-foil at $\theta_0 = 15°$ and $\theta_0 = 30°$ in the influence of inflow vortices are shown in Fig.12-17. The inflow vortices not only have impact on the magnitude of hydrodynamic coefficients but also on the phase angle of hydrodynamic coefficients. If the inflow vortices enlarge the magnitude of C_x, it will also enlarge the magnitude of C_y and C_m.
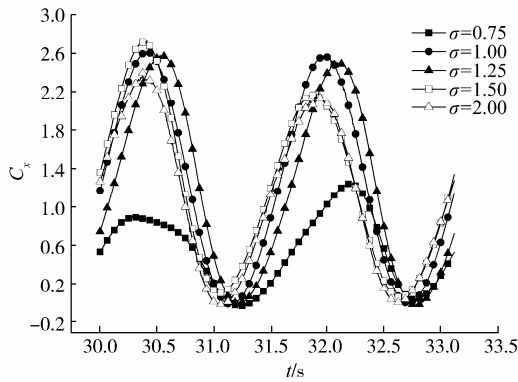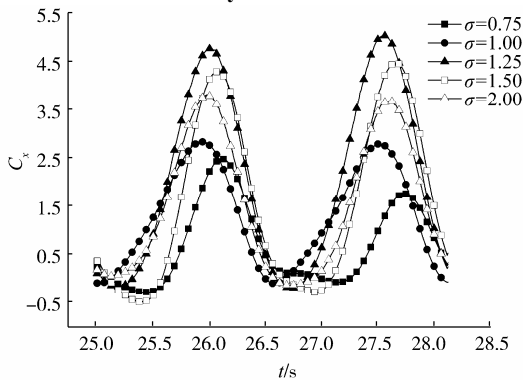
Fig.12 The thrust force coefficient varies in one cycle at θ=15°
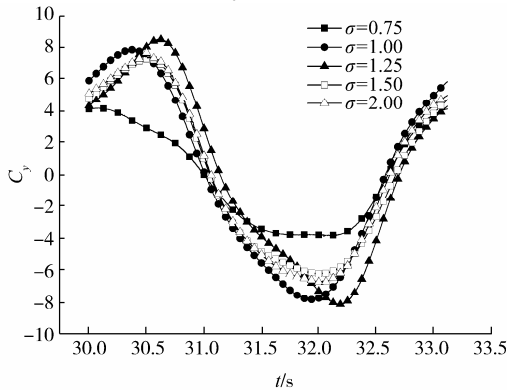
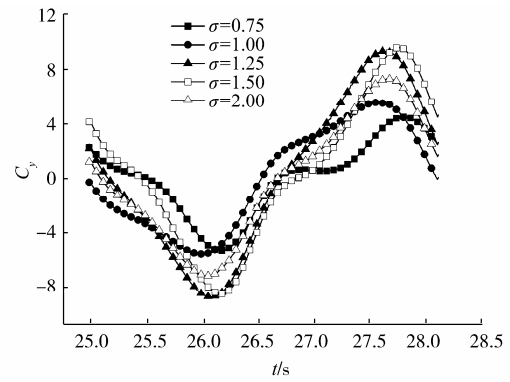**Fig.13 The lateral force coefficient varies in one cycle at θ=15°**
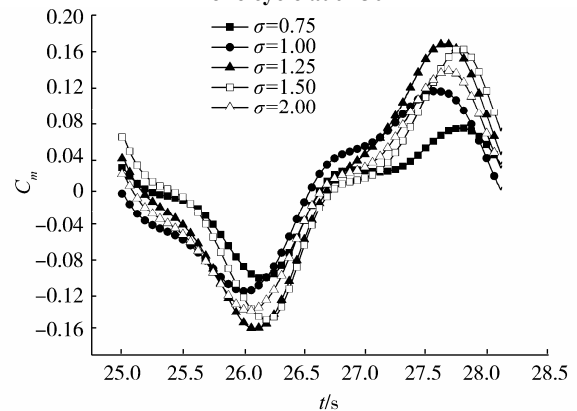

Fig.14 The moment force coefficient varies in one cycle at θ=15°

Fig.15 The thrust force coefficient varies in one cycle at θ=30°

Fig.16 The lateral force coefficient varies in one cycle at θ=30°

Fig.17 The moment force coefficient varies in one cycle at θ=30°

5 Conclusions

In this paper, the commercial CFD software FLUENT based on RANS equations was developed secondly to numerically calculate the hydrodynamic performance of flapping-foil in the influence of inflow vortices. What the results show is described as bellow.

1) The oscillating D-section cylinder can be used as a vortex-generator. The calculation method is available.

2) From the calculating results, four interaction modes which were proved by experiments mentioned above between inflow vortices and foil vortices are found.

3) Analyzing the hydrodynamic performance of flapping-foil in the influence of inflow vortices, the flapping-foil at mode 2 (The inflow vortex interacts with the same signed foil leading edge vortex and then they move forward independently). absorbs energy from inflow vortices. The mean thrust force coefficient of the flapping-foil at mode 4 (The inflow vortex interacts with the oppositely signed vortices generated by flapping-foil.) is increased largely, but the efficiency at this time is not high.

References

Anderson JM(1996). Vorticity control for efficiency propulsion. Massachusetts Institutes of Technology, Cambridge, 47-180.

Beal DN (2003). Propulsion through wake synchronization using flapping-foil. PhD, thesis, Massachusetts Institutes of Technology, Cambridge, 76-84.

Bearman PW (1984). Vortex shedding from oscillating bluff bodies. *Annual Review of Fluid Mechanics*, **16**, 195-222.

Gopalkrishnan R, Triantafyllou MS, Triantafyllou GS (1994). Active vorticity control in a shear flow using a flapping foil. *Journal of Fluid Mechanics*, **27**(4), 1-21.

Guglielmini L, Blondeaux P (2004). Propulsive efficiency of oscillating foils. *European Journal of Mechanics B/Fluids*, **23**, 255-278.

Liao Q, Dong GJ, Lu XY (2004). Vortex formation and force characteristic of a foil in the wake of a circular cylinder. *Journal of Fluids and Structures* ,**19**, 491-510.

Sarpkaya T (1979). Vortex-induced oscillations, a selective review. *Journal of Applied Mechanics*, **46**, 241-258.

Simmons JEL (1974). Phase-angle measurements between hot-wire signals in the turbulent wake of a two-dimensional bluff body. *Journal of Fluid Mechanics*, **64**, 599-609.

Song HJ, Wang Z, Yin XZ (2004). Numerical simulation on unsteady motion of 2D airfoil. *Journal of Hydrodynamics*, **19**(A)Supplement, 896-903.

Stansby PK (1976). The locking-on of vortex shedding due to the cross-stream vibration of circular cylinders in uniform and shear flows. *Journal of Fluid Mechanics*, **74**, 641-665.

Streitlien K, Triantafyllou GS (1996).Efficient foil propulsion through vortex control. *AIAA Journal*, **34**(11), 2315-2318.

Triantafyllou MS, Triantafyllou GS, Yue DKP (2000). Hydrodynamics of fishlike swimming. *Fluid Mech*, **32**, 33-53.

Wang FJ (2004). *The Analysis of computational fluid dynamics—The theory and application of CFD software*. Tsinghua University Press, Beijing, 120-126.

Wang J (2000). Vortex shedding and frequency selection in flapping flight. *J. Fluid Mech*, **410**, 323-341.

Williamson CHK, Roshko A (1988). Vortex formation in the wake of an oscillating cylinder. *Journal of Fluids and Structures*, **2**, 355-381.

Yang L, Su YM (2007). Hydrodynamic analysis of an oscillating tail-fin in viscous flows. *Journal of Harbin Engineering University*, **28**(10), 1073-1078.

Xi Zhang was born in 1985. He received the bachelor degree in Shipbuilding and Marine Engineering at Harbin Engineering University. His current research interests include CFD and bionic engineering.

Yu-min Su was born in 1960. He is a professor at the School of Shipbuilding Engineering, Harbin Engineering University. His current research interests include fluid dynamics and marine propeller design, system integration of underwater vehicles

Liang Yang was born in 1980. He received his Ph.D degree from Harbin Engineering University. His current research interests include CFD of ship and bionic engineering.

Zhao-li Wang was born in 1983. He received M.Sc in Design and Construction of Naval Architecture and Ocean Structure in 2008. Now he is working for the Ph.D degree in Engineering Mechanics at Harbin Engineering University.